Supporting Information

Chlorination Revisited: Does Cl^- Serve as a Catalyst in the Chlorination of Phenols?

Stephanie S. Lau,[†] Sonali M. Abraham,[†,‡] and A. Lynn Roberts*,[†]

[†] Department of Environmental Health and Engineering, Johns Hopkins University, 313 Ames Hall, 3400 North Charles Street, Baltimore, Maryland 21218, United States

[‡] Institute of the Environment and Sustainability, University of California, Los Angeles, La Kretz Hall, 619 Charles E. Young Drive East #300, Los Angeles, California 90024, United States

* Corresponding author contact information:

Phone: 410-516-4387; Fax: 410-516-8996; E-mail: lroberts@jhu.edu

Contains 31 pages, 1 reaction scheme, 2 tables, and 12 figures

Table of Contents

Acronyms

FAC: free available chlorine
2-CP: 2-chlorophenol
4-CP: 4-chlorophenol
2,4-DCP: 2,4-dichlorophenol
2,6-DCP: 2,6-dichlorophenol
TCP: 2,4,6-trichlorophenol

FAC speciation

The speciation diagram for free available chlorine (FAC) shown in Fig. 1 (main text) was constructed based on the following processes:

$H_2OCl^+ \rightleftharpoons HOCl + H^+$ $\quad pK_{a,\ H2OCl+} = -3$ to -4

$HOCl \rightleftharpoons OCl^- + H^+$ $\quad pK_{a,\ HOCl} = 7.54$

$HOCl + Cl^- + H^+ \rightleftharpoons Cl_{2\,(aq)} + H_2O$ $\quad \log K_{Cl2} = 2.72$

$2\ HOCl \rightleftharpoons Cl_2O_{(aq)} + H_2O$ $\quad \log K_{Cl2O} = -2.06$

Information about the different equilibrium constants, including the appropriate references, can be found in the main text.

Chemical reagents

2-Chlorophenol (≥ 98%), 2,6-dichlorophenol (99%), and 2,4-dichlorophenol (99%) were purchased from Acros Organics. Phenol (≥ 99%), sodium nitrate (≥ 99.0%), and potassium iodide (≥ 99.0%) were purchased from Sigma-Aldrich. 4-Chlorophenol (≥ 99%) and 2,4,6-trichlorophenol (98%) were purchased from Aldrich. Commercial sodium hypochlorite (NaOCl) solutions (5.65–6%), glacial acetic acid (certified ACS), methanol (Optima® LC/MS), sodium hydroxide (certified ACS pellets), and sodium chloride (certified ACS crystalline) were obtained from Fisher. Sodium thiosulfate pentahydrate (99.5–101.0%) was purchased from Alfa Aesar. Sodium bicarbonate, sodium dihydrogen phosphate, and disodium hydrogen phosphate (all ACS grade) were obtained from J. T. Baker. Nitric acid was acquired from EMD. Except for sodium chloride (see "NaCl recrystallization procedure" on p. S5), all the reagents were used without further purification.

Monitoring [FAC]

For each (chloro)phenol, [FAC] was monitored as a function of time at selected pH values to ensure that pseudo-first-order conditions ([FAC] ≈ $[FAC]_0$ ≈ constant) were maintained throughout the experiments. [FAC] was determined using a UV-visible spectrophotometric method adapted from ref. 1. Briefly, 2 mL of reaction solution was added to a glass vial containing 0.5 mL of 0.17 M potassium iodide (KI) solution. The FAC in the reaction solution stoichiometrically oxidized I^- to triiodide (I_3^-). The absorbance of I_3^- was monitored at 351 nm (ϵ = 26200 L mol^{-1} cm^{-1}) using a Shimadzu UV-1800 UV-visible spectrophotometer with a 1-cm path length. The concentration of I_3^- (and hence [FAC]) was then calculated using the Beer-Lambert law.

Control experiments conducted in the presence of each pH buffer employed (but in the absence of (chloro)phenols) revealed < 5% loss of [FAC] over 1.5 hours, a time in excess of the duration of most of our experiments (data not shown). Therefore, FAC was not consumed at appreciable rates through reactions with our pH buffers.

NaCl recrystallization procedure

To reduce bromide (Br^-) contamination, commercial sodium chloride (NaCl) was recrystallized in our laboratory using the following method: 35 g of NaCl was dissolved in 100 mL of Milli-Q water in a 500-mL beaker. The mixture was heated on a hot plate with occasional stirring until the NaCl had completely dissolved. The beaker was then removed from heat and the solution was allowed to cool to room temperature. NaCl crystals began to form as the solution cooled. Once the solution reached room temperature, the beaker was placed in an ice bath, whereupon more NaCl crystals formed. Once the solution reached temperature equilibrium with the ice slurry, acetone (100 mL) was slowly added to the beaker over 5 minutes. The NaCl solution turned cloudy as more crystals formed. The beaker was covered with aluminum foil and was stored at 4°C for ≥ 8 hours. Vacuum filtration was then used to separate the NaCl crystals from the acetone-water mixture while the mixture was still cold. The NaCl crystals were dried at 100°C for 30 minutes before weighing. The NaCl was recrystallized for a second time to further reduce the Br^- content.

Analysis by ion chromatography (IC) revealed that 0.780 μM of Br^- was present in a 30 mM NaCl solution prepared by dissolving the original (non-recrystallized) NaCl in water. Bromide was not detected in a 30 mM NaCl solution made using the twice-recrystallized NaCl (Br^- detection limit = 0.02 μM). Thus, the recrystallization procedure was effective in reducing the Br^- content in NaCl by ≥ 97%.

IC measurements were carried out using a Dionex ICS-2100 ion chromatography system with a Dionex AERS 500 Suppressor and an IonPac® AS18 anion-exchange column (4 × 250 mm) from Thermo Fisher Scientific. The eluent was 30 mM KOH, and analyses were performed at a column temperature of 30°C.

Data fitting procedure

The modeling approach described herein is similar to the processes described in refs. 2 and 3. Second-order rate constants were estimated via nonlinear least-squares regressions of the experimental data (k_{obs}) for (chloro)phenol decay using the computer program SigmaPlot 12.5 (Systat Software). Assuming that HOCl, Cl_2, and Cl_2O all influence the reaction kinetics of (chloro)phenols, the change in [(chloro)phenol]$_T$ over time can be expressed as

$$-\frac{d[ArOH]_T}{dt} = -\left(\frac{d[ArOH]}{dt} + \frac{d[ArO^-]}{dt}\right)$$
$$= k_{HOCl,\,ArOH}[HOCl][ArOH] + k_{HOCl,\,ArO^-}[HOCl][ArO^-]$$
$$+ k_{Cl_2,\,ArOH}[Cl_2][ArOH] + k_{Cl_2,\,ArO^-}[Cl_2][ArO^-]$$
$$+ k_{Cl_2O,\,ArOH}[Cl_2O][ArOH] + k_{Cl_2O,\,ArO^-}[Cl_2O][ArO^-] \quad (S1)$$

where ArOH and ArO^- represent the conjugate acid and phenolate forms, respectively, and $[ArOH]_T = [ArOH] + [ArO^-]$. As our experiments were conducted under pseudo-first-order conditions in which $[FAC] \approx [FAC]_0 \gg [(chloro)phenol]_o$, we can express eq. S1 as

$$-\frac{d[ArOH]_T}{dt} = k_{obs}\,[ArOH]_T \quad (S2)$$

The pseudo-first-order coefficient (k_{obs}) can be written as

$$k_{obs} = k_{HOCl,\,ArOH}\,[HOCl]\,f_{ArOH} + k_{HOCl,\,ArO^-}\,[HOCl]\,f_{ArO^-}$$
$$+ k_{Cl_2,\,ArOH}\,[Cl_2]\,f_{ArOH} + k_{Cl_2,\,ArO^-}\,[Cl_2]\,f_{ArO^-}$$
$$+ k_{Cl_2O,\,ArOH}\,[Cl_2O]\,f_{ArOH} + k_{Cl_2O,\,ArO^-}\,[Cl_2O]\,f_{ArO^-} \quad (S3)$$

where f_{ArOH} and f_{ArO^-} represent the fractions of (chloro)phenol in the conjugate acid (ArOH) and phenolate (ArO^-) forms, respectively, and $f_{ArO^-} = (1 - f_{ArOH})$.

$$f_{ArOH} = \frac{[ArOH]}{[ArOH]+[ArO^-]} = \frac{1}{1+(K_a/[H^+])} \quad (S4)$$

$[Cl_2]$ and $[Cl_2O]$ in eq. S3 can be rewritten in terms of [HOCl]:

$$k_{obs} = k_{HOCl,\,ArOH}[HOCl]f_{ArOH} + k_{HOCl,\,ArO^-}[HOCl]f_{ArO^-}$$
$$+ k_{Cl_2,\,ArOH} K_{Cl_2} [HOCl][Cl^-][H^+]f_{ArOH} + k_{Cl_2,\,ArO^-} K_{Cl_2} [HOCl][Cl^-][H^+]f_{ArO^-}$$
$$+ k_{Cl_2O,\,ArOH} K_{Cl_2O} [HOCl]^2 f_{ArOH} + k_{Cl_2O,\,ArO^-} K_{Cl_2O} [HOCl]^2 f_{ArO^-} \quad (S5)$$

where K_{Cl_2} and K_{Cl_2O} are the equilibrium constants for the formation of Cl_2 and Cl_2O, respectively. The values of $\log K_{Cl_2}$ and $\log K_{Cl_2O}$ are given on p. S3 and in the main text.

Equation S5 reflects all the reactions between FAC and (chloro)phenols considered in this study. It is necessary to check whether all the terms are required to fit the experimental data to avoid over-parameterizing the model. The fitting procedure minimizes the sums of squares between the experimental log k_{obs} data and the model predictions, and only one parameter (i.e., one second-order rate constant) is fitted at any given time. Uncertainties in the second-order rate constants indicate the 95% confidence intervals calculated by SigmaPlot 12.5.

The modeling procedure for phenol will be described in detail to illustrate our data fitting approach. We first modeled the no-added-chloride data at pH > 9 (where k_{obs} decreases with increasing pH) with the assumption that the HOCl/ArO^- reaction is the only one important at high pH. We fixed all other second-order rate constants in eq. S5 at zero and computed $k_{HOCl,\,ArO^-}$, which we estimated to be 2.61 (± 0.26) × 10^4 M^{-1} s^{-1} (Fig. S1a). With $k_{HOCl,\,ArO^-}$ constrained to this value, we modeled the log k_{obs} vs. log $[HOCl]_0$ data from reaction order experiments at pH 4.7 by assuming that Cl_2O/ArOH is the dominant reaction at low pH. Our initial estimate for $k_{Cl_2O,\,ArOH}$ was 3.61 (± 0.31) × 10^5 M^{-1} s^{-1} (Fig. S1b). Next, we constrained both $k_{HOCl,\,ArO^-}$ and $k_{Cl_2O,\,ArOH}$ to their estimated values while modeling the 5-mM-added-Cl^- data at pH < 5.5 to compute $k_{Cl_2,\,ArOH}$. Our initial estimate of $k_{Cl_2,\,ArOH}$ was 8.47 (± 1.40) × 10^4 M^{-1} s^{-1} (Fig. S1c). As ion chromatographic measurements revealed that, for phenol, 0.17 mM Cl^- was present in reactors without added NaCl (see later discussion under “Chloride in FAC

solutions: Origin and measurement via ion chromatography" on p. S15-S16), the Cl_2/ArOH reaction could be important even in the absence of added Cl^-. Thus, we might have overestimated $k_{Cl_2O,\,ArOH}$ by not considering the Cl_2/ArOH reaction when modeling the log k_{obs} vs. log $[HOCl]_0$ data at pH 4.7. We modeled the same data set again, but this time we constrained $k_{Cl_2,\,ArOH}$ = 8.47 (± 1.40) × 10^4 M^{-1} s^{-1} and $[Cl^-]$ = 0.17 mM while computing a new estimate for $k_{Cl_2O,\,ArOH}$ (Fig. S1d). Afterwards, we modeled the entire 5-mM-added-Cl^- data set to compute $k_{Cl_2,\,ArO^-}$ with $k_{HOCl,\,ArO^-}$, $k_{Cl_2O,\,ArOH}$, and $k_{Cl_2,\,ArOH}$ constrained to their previously estimated values. The initial estimate for $k_{Cl_2,\,ArO^-}$ was 1.31 (± 0.78) × 10^9 M^{-1} s^{-1} (Fig. S1e). With $k_{Cl_2,\,ArO^-}$ constrained, we then sequentially estimated $k_{Cl_2O,\,ArOH}$ and $k_{Cl_2,\,ArOH}$ again. We repeated the process a few more times until we obtained the best qualitative fit to the log k_{obs} vs. pH data (Fig. S1f). The best-fit estimates of second-order rate constants are as follows: $k_{HOCl,\,ArO^-}$ = 2.61 (± 0.26) × 10^4 M^{-1} s^{-1}, $k_{Cl_2,\,ArOH}$ = 8.92 (± 0.98) × 10^4 M^{-1} s^{-1}, $k_{Cl_2,\,ArO^-}$ = 2.61 (± 0.50) × 10^9 M^{-1} s^{-1}, and $k_{Cl_2O,\,ArOH}$ = 9.02 (± 3.06) × 10^4 M^{-1} s^{-1}. We did not include the terms for $k_{HOCl,\,ArOH}$ and $k_{Cl_2O,\,ArO^-}$ in the final model for phenol (eq. 6 in main text) because they did not provide any improvement to the fit to the experimental data.

The iterative data fitting processes for the other chlorophenols are similar to the one described for phenol. Although the final models for the six (chloro)phenols are different, we followed these general data fitting principles:

1. $k_{HOCl,\,ArO^-}$ is estimated from no-added-chloride data at high pH
2. $k_{Cl_2O,\,ArOH}$ is estimated from log k_{obs} vs. log $[HOCl]_0$ data at low pH
3. $k_{Cl_2,\,ArOH}$ (if included) is estimated from 3- or 5-mM-added-Cl^- data at low pH
4. $k_{Cl_2,\,ArO^-}$ is estimated from the entire 3- or 5-mM-added-Cl^- data set

5. $k_{Cl_2O,\,ArO^-}$ (if included) is estimated from the entire no-added-chloride data set

Using our model for phenol (eq. 6 in main text), we also calculated a value for [Cl^-] in the no-NaCl-added reactors that is independent of ion chromatographic measurements. After computing the initial estimates of $k_{HOCl,\,ArO^-}$, $k_{Cl_2O,\,ArOH}$, and $k_{Cl_2,\,ArOH}$, we constrained these rate constants and used [Cl^-] as a fitting parameter for the no-added-chloride data at pH < 4.5 (where k_{obs} increases with decreasing pH). When computing $k_{Cl_2O,\,ArOH}$ for a second time, we fixed [Cl^-] at the previously estimated value. The iterative data fitting proceeded as described above. For phenol ($[FAC]_0$ = 125 μM), the final estimate of [Cl^-] in reactors without NaCl is 0.22 ± 0.03 mM. This calculated value of [Cl^-] is close to the measured [Cl^-] value (0.17 mM).

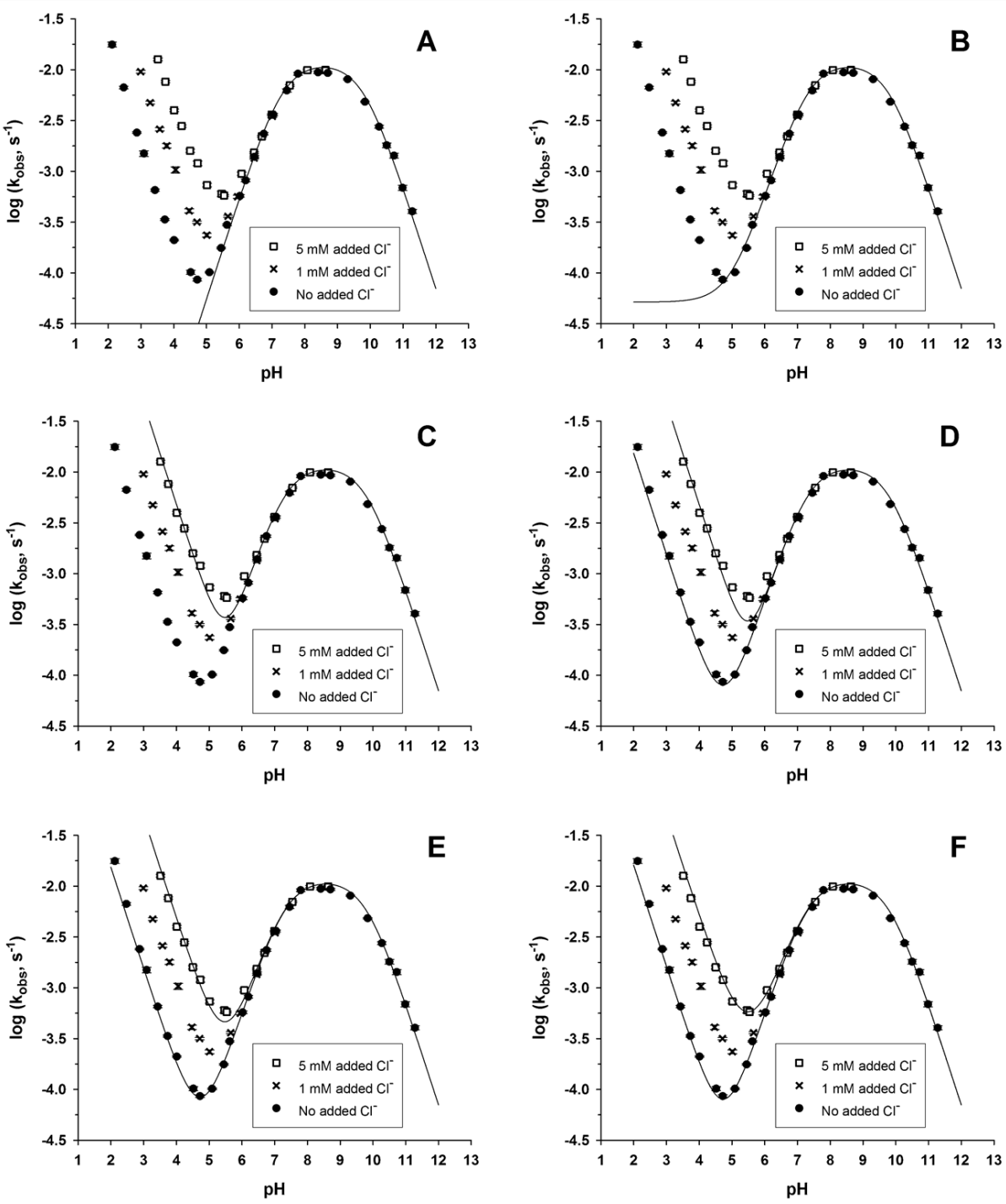

Figure S1. Plots of log k_{obs} vs. pH for phenol showing the model fit at various stages of the iterative data fitting process: **(A)** HOCl/ArO^--only model; **(B)** both HOCl and Cl_2O were considered; **(C)** fitting $k_{Cl2,\ ArOH}$ while constraining $k_{HOCl,\ ArO-}$ and $k_{Cl2O,\ ArOH}$; **(D)** fitting $k_{Cl2O,\ ArOH}$ while $k_{Cl2,\ ArOH}$ and $k_{HOCl,\ ArO-}$ were constrained; **(E)** fitting $k_{Cl2,\ ArO-}$ while all other second-order rate constants were constrained; and **(F)** the final model fit. Note that the 1-mM-added-Cl^- data were not used in the data fitting process.

We also used the program Scientist 3.0 (Micromath) to predict the concentrations of all six (chloro)phenols (parent compounds and products alike) as a function of time. We input the differential rate laws for all (chloro)phenols according to Scheme 1, and we used the best-fit estimates of second-order rate constants listed in Table 1 (main text) to calculate the pseudo-first-order rate coefficients (k_{calc}) we would expect for a given value of $[FAC]_0$. Those k_{calc} values are represented by k_A, k_B, k_C, k_D, k_E, and k_F in the Scientist 3.0 model. Phenol can be chlorinated to form either 2-CP or 4-CP, while 2-CP can be chlorinated to form 2,4-DCP or 2,6-DCP. As we were unable to determine k_{AB}, k_{AC}, k_{BD}, k_{BE} experimentally, we treated them as fitting parameters (keeping in mind that $k_{AB} + k_{AC} = k_A$ and $k_{BD} + k_{BE} = k_B$) while all the other rate coefficients were constrained. The concentration profiles of the (chloro)phenols predicted by our model from the chlorination of phenol are illustrated in Fig. S2.

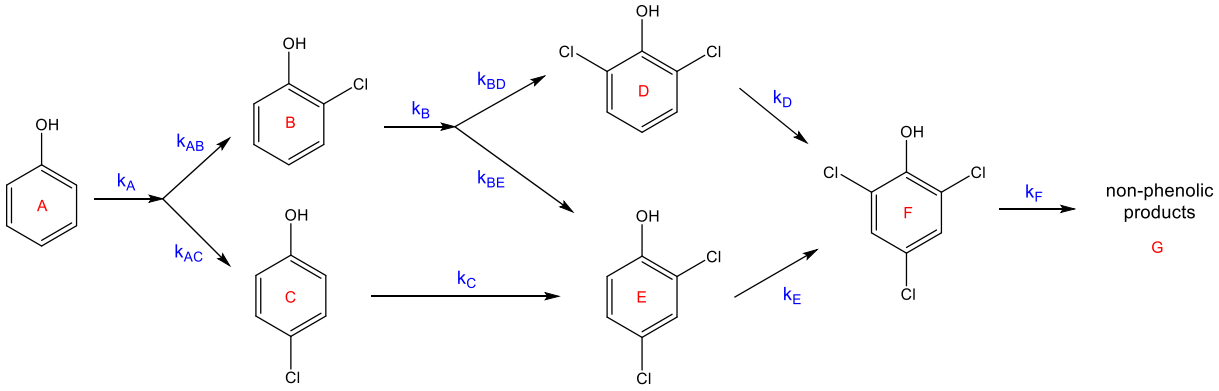

Scheme S1. Reaction pathway for the chlorination of phenol.

Examples of reaction time courses for phenol showing the predicted vs. measured concentrations of reaction products

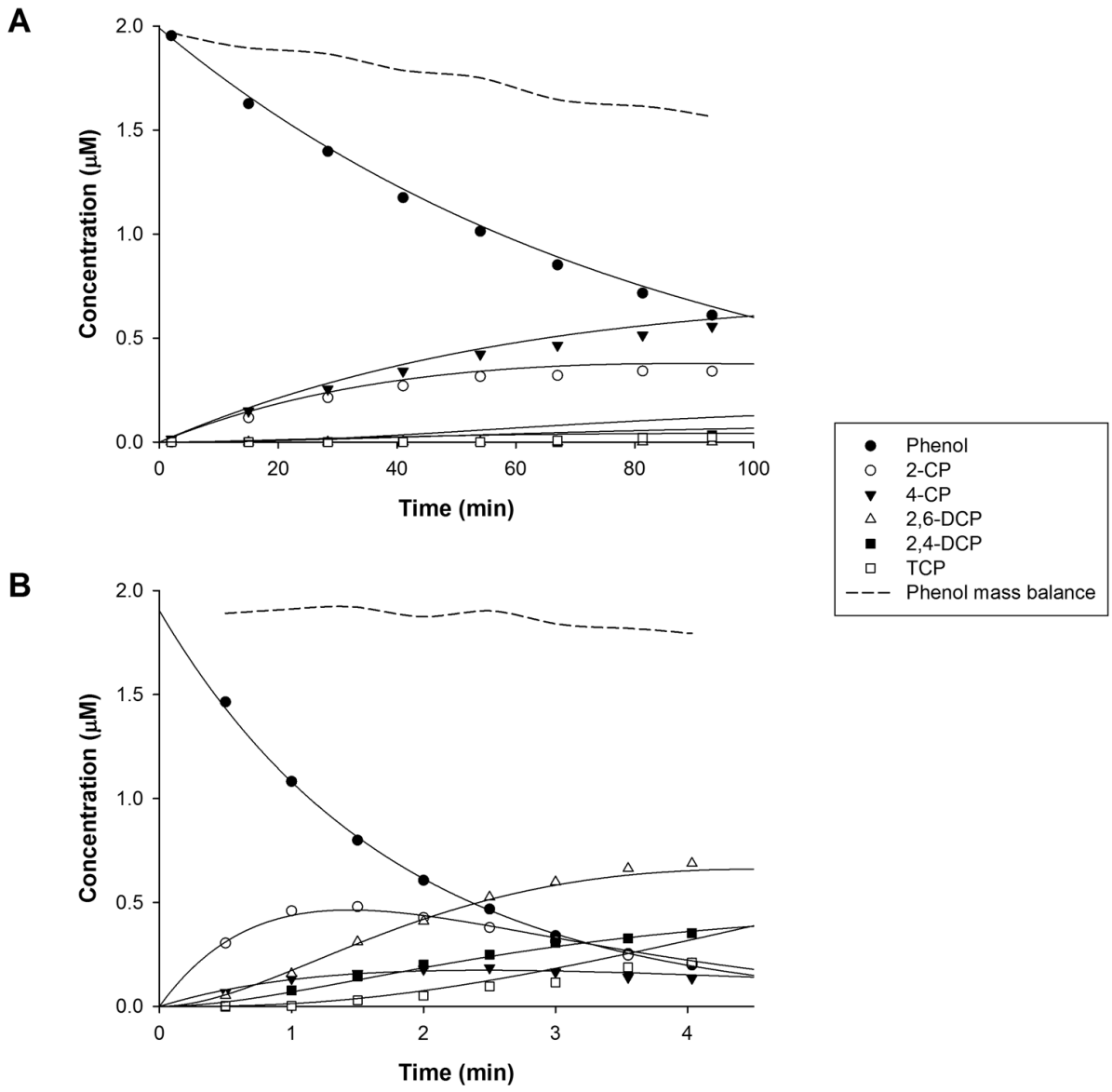

Figure S2. Typical reaction time courses for reactors spiked with phenol at **(A)** pH 4.0 and **(B)** pH 8.4. Concentrations of the reaction products were also monitored. Experimental conditions: $[FAC]_0$ = 125 μM, $[phenol]_0$ = 2 μM, ionic strength = 0.1 M, [pH buffer] = 10 mM, T = 25°C. No NaCl was added. Solid lines are model predictions based on the second-order rate constants in Table 1 and eq. 6 (main text). Dashed lines represent the phenol mass balance (calculated as [phenol] + [2-CP] + [4-CP] + [2,6-DCP] + [2,4-DCP] + [TCP]).

Sample data from phenol chlorination experiments

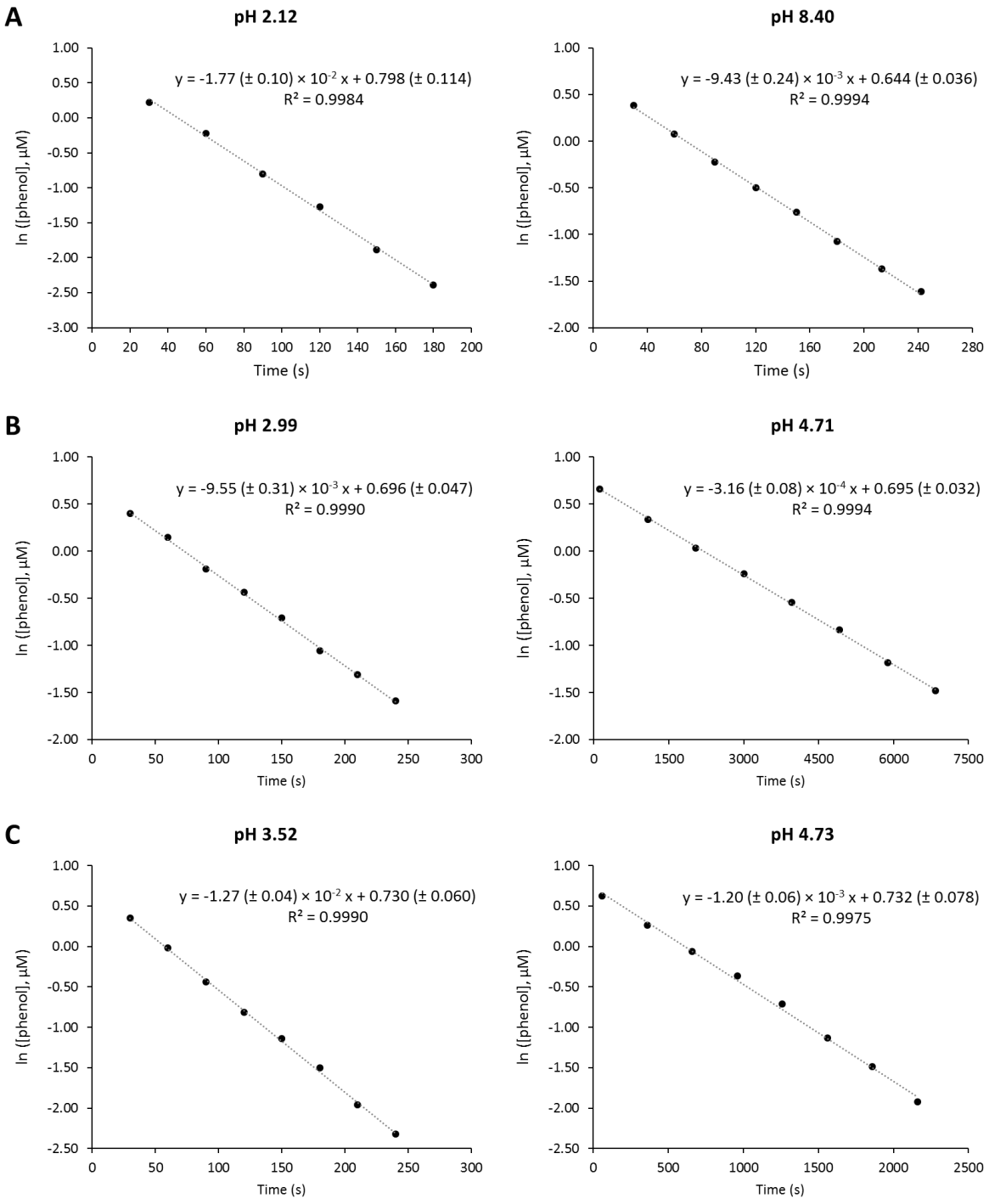

Fig. S3. Linear regressions of ln[phenol] vs. time data for selected reactors with **(A)** no Cl^- added, **(B)** $[Cl^-]_{added}$ = 1 mM, and **(C)** $[Cl^-]_{added}$ = 5 mM. Reaction conditions: $[FAC]_0$ = 125 µM, $[phenol]_0$ = 2 µM, [pH buffer] = 10 mM, ionic strength = 0.1 M, T = 25°C. Uncertainties in the slopes and y-intercepts indicate 95% confidence intervals.

Plots of log k_{obs} vs. pH for 2-CP and 2,6-DCP

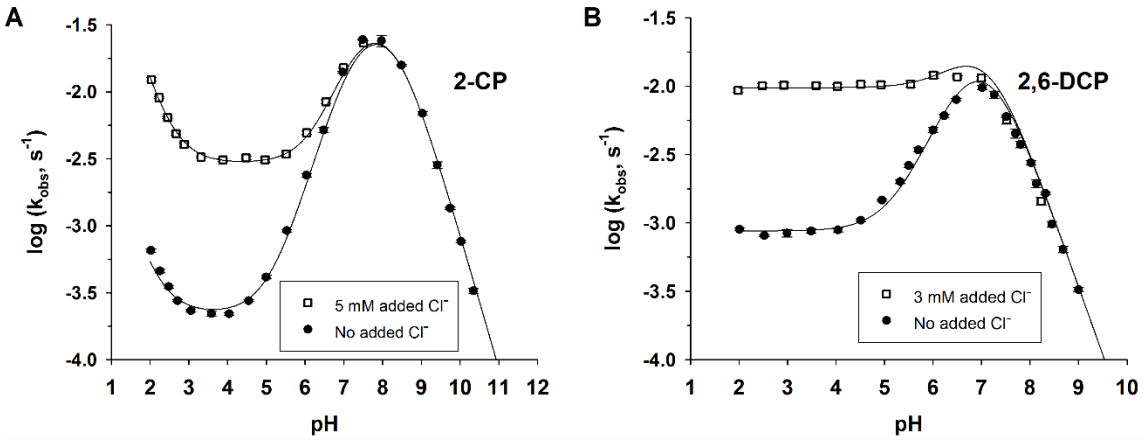

Figure S4. Pseudo-first-order rate coefficients (k_{obs}) as a function of pH for **(A)** 2-CP and **(B)** 2,6-DCP. Reaction conditions: $[FAC]_0$ = 125 μM, $[chlorophenol]_0$ = 2 μM; $[NaCl]_0$ = 3 or 5 mM (if added), ionic strength = 0.1 M, T = 25°C. Error bars indicate 95% confidence intervals (smaller than symbols if not shown). Solid lines are fits to a model of the form of eq. 6 (2-CP) or eq. 8 (2,6-DCP) in the main text.

Chloride in FAC solutions: Origin and measurement via ion chromatography

Sodium hypochlorite (NaOCl) is typically manufactured by bubbling gaseous Cl_2 into water and then adding two moles of NaOH for every 1 mol of Cl_2,[4] i.e.

$$Cl_{2\,(aq)} + 2\,NaOH \rightarrow NaOCl + NaCl + H_2O$$

A solution of NaOCl made via the above process ought to contain equimolar concentrations of $[Cl^-]$ and $[OCl^-]_T$. Nonetheless, sodium hypochlorite is known to degrade over a time scale of months, even when the concentrated stock solution is stored in the dark at 4°C. Rather than relying on deduction to assess the chloride concentration in our FAC solutions, we opted to measure it via ion chromatography (IC).

Our approach to Cl^- measurements was similar to that used by Cherney et al.[5] First, the commercial NaOCl stock solution was standardized iodometrically according to Standard Methods 4500-Cl B.[6] After diluting the NaOCl stock solution with Milli-Q water to the desired concentration, a molar excess of sodium sulfite (Na_2SO_3) was added to reduce all chlorinating agents to Cl^-. Then, the total chloride ($[Cl^-]_{total}$) in the solution was determined by IC. As the concentration of FAC initially present in the FAC solution ($[FAC]_0$) was known, we could calculate the concentration of chloride contributed by the NaOCl stock solution by difference: $[Cl^-]$ in FAC solution = $[Cl^-]_{total} - [FAC]_0$. The concentration of Cl^- in our FAC solutions as a function of $[FAC]_0$ is shown in Fig. S5.

IC measurements were carried out using a Dionex ICS-2100 ion chromatography system with a Dionex AERS 500 Suppressor and an IonPac® AS18 anion-exchange column (4 × 250 mm) from Thermo Fisher Scientific. The eluent was 30 mM KOH, and analyses were performed at a column temperature of 30°C.

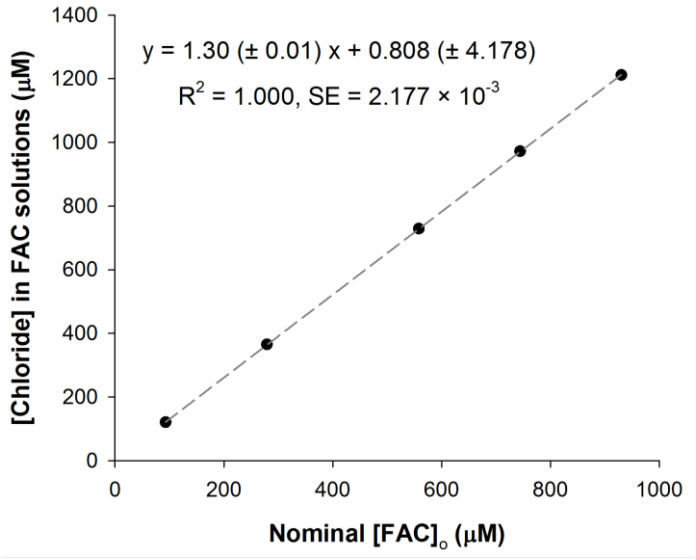

Figure S5. Concentration of chloride contributed by the NaOCl stock solution as a function of nominal $[FAC]_0$. The FAC solutions were made by diluting a commercial NaOCl stock with Milli-Q water. No other reagents were added to the FAC solutions. Uncertainties indicate 95% confidence intervals.

Plots of log k_{obs} vs. log $[HOCl]_0$ for all chlorophenols

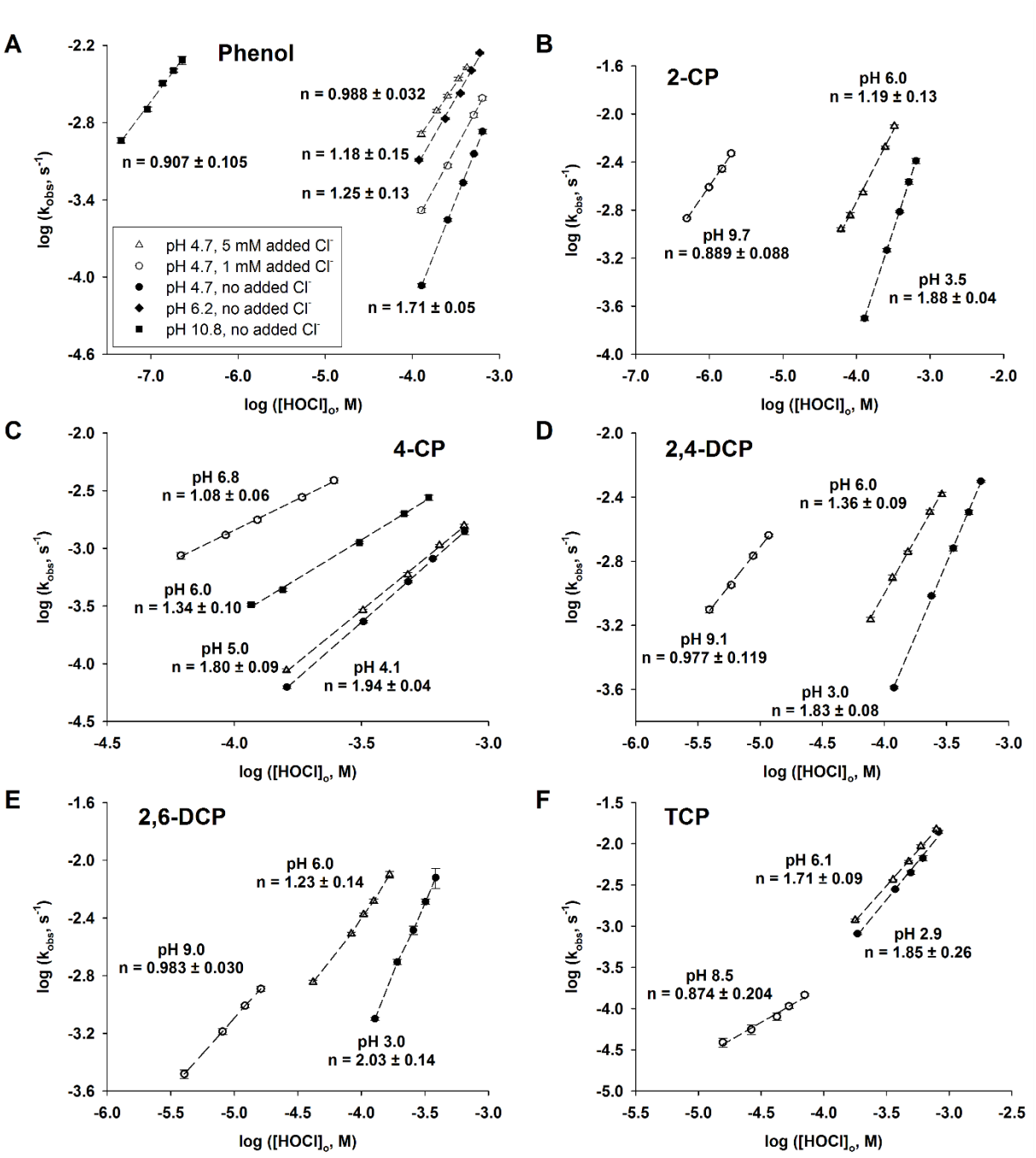

Figure S6. Plots of log k_{obs} vs. log $[HOCl]_0$ at different pH values for **(A)** phenol, **(B)** 2-CP, **(C)** 4-CP, **(D)** 2,4-DCP, **(E)** 2,6-DCP, and **(F)** TCP. Reaction conditions: $[chlorophenol]_0$ = 2 μM; [pH buffer] = 10 mM; ionic strength = 0.1 M; T = 25°C, $[FAC]_0$ = 125–640 μM for phenol; 125–520 μM for 2-CP; 80–805 μM for 4-CP; 80–600 μM for 2,4-DCP; 43–520 μM for 2,6-DCP; 185–825 μM for TCP. No NaCl was added unless otherwise indicated. Uncertainties in the slopes (*n*) denote 95% confidence intervals.

Reaction order in [FAC]

The reaction order (*n*) in [FAC] can be calculated using the second-order rate constants listed in Table 1 (see main text). The derivation of calculated *n* (n_{calc}) for phenol, 2-CP, and 4-CP is shown below.

The final model for phenol, 2-CP, and 4-CP reactivity in the presence of FAC is

$$k_{obs} = k_{HOCl,\,ArO^-}[HOCl]\,f_{ArO^-} + k_{Cl_2O,\,ArOH}\,[Cl_2O]\,f_{ArOH} + k_{Cl_2,\,ArOH}\,[Cl_2]\,f_{ArOH} + k_{Cl_2,\,ArO^-}[Cl_2]\,f_{ArO^-} \quad \text{(S6)}$$

where k_{obs} represents the pseudo-first-order rate constant determined from kinetic experiments; f_{ArOH} and f_{ArO^-} represent the fractions of (chloro)phenol in the conjugate acid (ArOH) and phenolate (ArO^-) forms, respectively.

Substituting known quantities for $[Cl_2]$ and $[Cl_2O]$ into eq. S6:

$$k_{obs} = k_{HOCl,\,ArO^-}[HOCl]\,f_{ArO^-} + k_{Cl_2O,\,ArOH}\left(K_{Cl_2O}\,[HOCl]^2\right)f_{ArOH} + k_{Cl_2,\,ArOH}\left(K_{Cl_2}[HOCl][Cl^-][H^+]\right)f_{ArOH} + k_{Cl_2,\,ArO^-}\left(K_{Cl_2}[HOCl][Cl^-][H^+]\right)f_{ArO^-} \quad \text{(S7)}$$

Measurements by ion chromatography (IC) showed that the FAC solutions in our experiments contained roughly equimolar concentrations of [FAC] and $[Cl^-]$. As [HOCl] ≈ [FAC] at pH ≤ 6.5, we can substitute $[Cl^-]$ for [HOCl] in eq. S7 to obtain the following:

$$k_{obs} = k_{HOCl,\,ArO^-}[HOCl]\,f_{ArO^-} + k_{Cl_2O,\,ArOH}\left(K_{Cl_2O}\,[HOCl]^2\right)f_{ArOH} + k_{Cl_2,\,ArOH}\left(K_{Cl_2}\,[HOCl]^2[H^+]\right)f_{ArOH} + k_{Cl_2,\,ArO^-}\left(K_{Cl_2}\,[HOCl]^2[H^+]\right)f_{ArO^-} \quad \text{(S8)}$$

Factoring out [HOCl] yields eq. S9:

$$k_{obs} = [HOCl]\,(k_{HOCl,\,ArO^-}\,f_{ArO^-} + k_{Cl_2O,\,ArOH}\,K_{Cl_2O}[HOCl]\,f_{ArOH} + k_{Cl_2,\,ArOH}\,K_{Cl_2}[HOCl][H^+]\,f_{ArOH} + k_{Cl_2,\,ArO^-}\,K_{Cl_2}[HOCl][H^+]\,f_{ArO^-}) \quad \text{(S9)}$$

Taking the log of both sides of eq. S9:

$$\log k_{obs} = \log [HOCl] + \log (k_{HOCl,\,ArO^-} f_{ArO^-} + k_{Cl_2O,\,ArOH} K_{Cl_2O}[HOCl] f_{ArOH} + k_{Cl_2,\,ArOH} K_{Cl_2}[HOCl][H^+] f_{ArOH} + k_{Cl_2,\,ArO^-} K_{Cl_2}[HOCl][H^+] f_{ArO^-}) \quad (S10)$$

Grouping the constants in eq. S10 together yields the following:

$$\log k_{obs} = \log [HOCl] + \log (C_1[HOCl] + C_2) \quad (S11)$$

where $C_1 = k_{Cl_2O,\,ArOH} K_{Cl_2O} f_{ArOH} + k_{Cl_2,\,ArOH} K_{Cl_2}[H^+] f_{ArOH} + k_{Cl_2,\,ArO^-} K_{Cl_2}[H^+] f_{ArO^-}$ and $C_2 = k_{HOCl,\,ArO^-} f_{ArO^-}$

The definition of n_{calc} is the slope of the derivative of log k_{obs} vs. the derivative of log [FAC]:

$$n_{calc} = \frac{d(\log k_{obs})}{d(\log [FAC])} \quad (S12)$$

Under the reaction conditions employed in this study, [FAC] can be approximated as the sum of [HOCl] and [OCl^-]:

$$[FAC] \approx [HOCl] + [OCl^-] = [HOCl]\left(1 + \frac{K_a}{[H^+]}\right) \quad (S13)$$

Taking the log of both sides of eq. S13:

$$\log [FAC] = \log [HOCl] + \log\left(1 + \frac{K_a}{[H^+]}\right) \quad (S14)$$

Rearranging eq. S14 and then taking the derivative of both sides yield the following:

$$\frac{d(\log [FAC])}{d(\log [HOCl])} = 1 \quad (S15)$$

which is equivalent to eq. S16:

$$d(\log [FAC]) = d(\log [HOCl]) \quad (S16)$$

Thus, eq. S12 can be written as

$$\therefore\ \mathrm{n_{calc}} = \frac{d(\log\ \mathrm{k_{obs}})}{d(\log\,[\mathrm{FAC}])} = \frac{d(\log\ \mathrm{k_{obs}})}{d(\log\ [\mathrm{HOCl}])} \tag{S17}$$

Substituting eq. S11 into eq. S17 leads to the following expressions for n_{calc}:

$$\mathrm{n_{calc}} = \frac{d(\log\ \mathrm{k_{obs}})}{d(\log\ [\mathrm{HOCl}])}$$

$$= \frac{d(\log\,[\mathrm{HOCl}])}{d(\log\,[\mathrm{HOCl}])} + \frac{d}{d(\log\ [\mathrm{HOCl}])}(\log\,(\mathrm{C_1}[\mathrm{HOCl}] + \mathrm{C_2})) \tag{S18}$$

$$\mathrm{n_{calc}} = 1 + \frac{d}{d(\log\ [\mathrm{HOCl}])}(\log\,(\mathrm{C_1}[\mathrm{HOCl}] + \mathrm{C_2})) \tag{S19}$$

Use the chain rule to evaluate $\frac{d}{d(\log\ [\mathrm{HOCl}])}(\log\,(\mathrm{C_1}[\mathrm{HOCl}] + \mathrm{C_2}))$ in eq. S19:

$$\frac{d}{d(\log\,[\mathrm{HOCl}])}(\log\,(\mathrm{C_1}[\mathrm{HOCl}] + \mathrm{C_2})) = \frac{d([\mathrm{HOCl}])}{d(\log\,[\mathrm{HOCl}])}\ \frac{d}{d([\mathrm{HOCl}])}(\log\,(\mathrm{C_1}[\mathrm{HOCl}] + \mathrm{C_2}))$$

$$= [\mathrm{HOCl}]\left(\frac{\mathrm{C_1}}{\mathrm{C_1}[\mathrm{HOCl}] + \mathrm{C_2}}\right) \tag{S20}$$

Substituting eq. S20 into eq. S19:

$$\mathrm{n_{calc}} = 1 + \frac{d}{d(\log\ [\mathrm{HOCl}])}(\log\,(\mathrm{C_1}[\mathrm{HOCl}] + \mathrm{C_2})) = 1 + [\mathrm{HOCl}]\left(\frac{\mathrm{C_1}}{\mathrm{C_1}[\mathrm{HOCl}] + \mathrm{C_2}}\right) \tag{S21}$$

Rearranging eq. S21 yields the following expression for n_{calc}:

$$\mathrm{n_{calc}} = \frac{2\ \mathrm{C_1}[\mathrm{HOCl}] + \mathrm{C_2}}{\mathrm{C_1}[\mathrm{HOCl}] + \mathrm{C_2}} \tag{S22}$$

Multiplying the numerator and denominator in eq. S22 by [HOCl] leads to eq. S23:

$$\mathrm{n_{calc}} = \frac{2\ \mathrm{C_1}[\mathrm{HOCl}]^2 + \mathrm{C_2}[\mathrm{HOCl}]}{\mathrm{C_1}[\mathrm{HOCl}]^2 + \mathrm{C_2}[\mathrm{HOCl}]} \tag{S23}$$

Replacing C_1 and C_2 in eq. S23 with their actual values:

$$n_{calc} = \frac{\mathbf{2}\left(k_{Cl_2O,\,ArOH}\,K_{Cl_2O}\,f_{ArOH} + k_{Cl_2,\,ArOH}\,K_{Cl_2}[H^+]\,f_{ArOH} + k_{Cl_2,\,ArO^-}\,K_{Cl_2}[H^+]\,f_{ArO^-}\right)[HOCl]^2 + k_{HOCl,\,ArO^-}\,f_{ArO^-}\,[HOCl]}{\left(k_{Cl_2O,\,ArOH}\,K_{Cl_2O}\,f_{ArOH} + k_{Cl_2,\,ArOH}\,K_{Cl_2}[H^+]\,f_{ArOH} + k_{Cl_2,\,ArO^-}\,K_{Cl_2}[H^+]\,f_{ArO^-}\right)[HOCl]^2 + k_{HOCl,\,ArO^-}\,f_{ArO^-}\,[HOCl]} \quad \text{(S24)}$$

Substituting $[Cl_2]$ and $[Cl_2O]$ into eq. S24 (and noting that $[Cl^-] \approx [HOCl]$ at pH $\leq$ 6.5):

$$n_{calc} = \frac{\mathbf{2}\,k_{Cl_2O,\,ArOH}\,[Cl_2O]\,f_{ArOH} + \mathbf{2}\,k_{HOCl,\,ArO^-}[HOCl]\,f_{ArO^-} + \mathbf{2}\,k_{Cl_2,\,ArOH}\,[Cl_2]\,f_{ArOH} + k_{Cl_2,\,ArO^-}[Cl_2]\,f_{ArO^-}}{k_{Cl_2O,\,ArOH}\,[Cl_2O]\,f_{ArOH} + k_{HOCl,\,ArO^-}[HOCl]\,f_{ArO^-} + k_{Cl_2,\,ArOH}\,[Cl_2]\,f_{ArOH} + k_{Cl_2,\,ArO^-}[Cl_2]\,f_{ArO^-}} \quad \text{(S25)}$$

As can be seen from eqs. S24 and S25, k_{obs} will show a second-order dependence on [HOCl] when either Cl_2 or Cl_2O is the dominant chlorinating agent. This is due to the FAC solutions used in our experiments being close to equimolar in [FAC] and [Cl^-].

The close agreement between the experimental *n* values and the calculated *n* values (n_{calc}) for phenol (Table S1) and 4-CP (Table S2) supports our assertion that Cl_2 is the predominant chlorinating agent for these compounds at low pH.

Table S1. Experimental reaction orders (*n*) and calculated reaction orders (n_{calc}) in [HOCl] for phenol in the absence of added Cl^-. Uncertainties indicate 95% confidence intervals.

pH	Range of $[FAC]_o$ (μM)	Experimental *n*	Range of n_{calc}	Average n_{calc}
4.7	125 – 640	1.71 ± 0.05	1.64 – 1.90	1.81
6.2	125 – 640	1.18 ± 0.15	1.02 – 1.11	1.07
10.8	125 – 640	0.907 ± 0.105	1.00 – 1.00	1.00

Table S2. Experimental reaction orders (*n*) and calculated reaction orders (n_{calc}) in [HOCl] for 4-CP in the absence of added Cl^-. Uncertainties indicate 95% confidence intervals.

pH	Range of $[FAC]_o$ (μM)	Experimental *n*	Range of n_{calc}	Average n_{calc}
4.1	160 – 805	1.94 ± 0.04	1.93 – 1.98	1.97
5.0	160 – 805	1.80 ± 0.09	1.59 – 1.88	1.78
6.0	120 – 610	1.34 ± 0.10	1.09 – 1.34	1.21
6.8	80 – 320	1.08 ± 0.06	1.01 – 1.04	1.02

Reaction order in [chlorophenol]

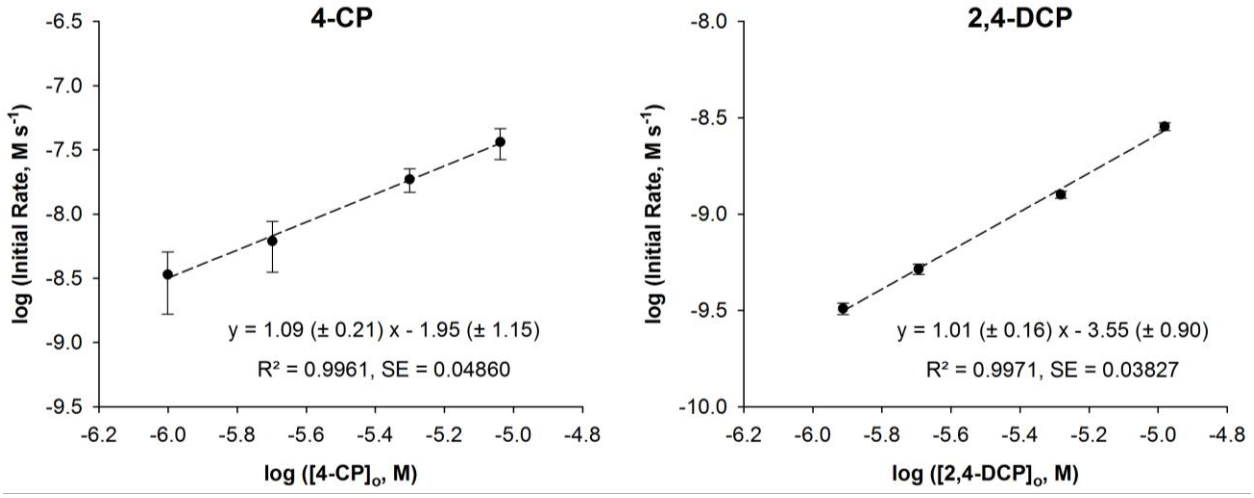

Figure S7. Initial chlorination rates as a function of initial (chloro)phenol concentrations for 4-CP and 2,4-DCP. Reaction conditions: [acetate buffer] = 10 mM, ionic strength = 0.1 M, T = 25°C. For 4-CP, pH = 5.0, $[FAC]_0$ = 330 μM, $[4\text{-CP}]_0$ = 1–10 μM. For 2,4-DCP, pH = 4.1, $[FAC]_0$ = 120 μM, $[2,4\text{-DCP}]_0$ = 1–9 μM. Error bars indicate 95% confidence intervals.

Effects of acetate buffer concentration on k_{obs} for TCP

Sodium acetate buffer increases the chlorination rate of 2,4,6-trichlorophenol (TCP) at pH > 2.8 (Fig. S8). This acetate buffer catalysis effect has been attributed to the formation of acetyl hypochlorite ($CH_3C(O)OCl$) from the reaction of HOCl with acetic acid.[7-11]

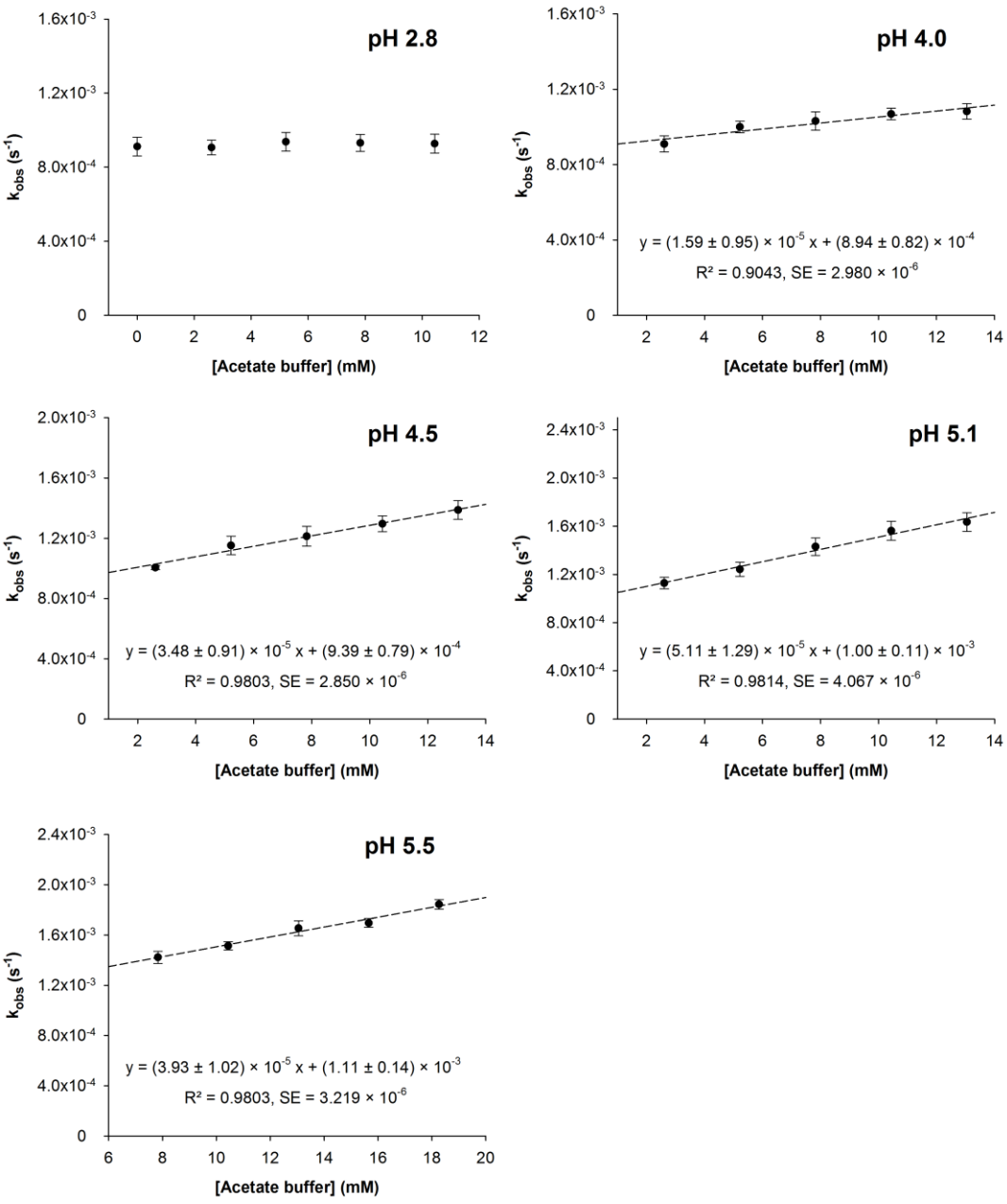

Figure S8. Chlorination rate constants (k_{obs}) as a function of acetate buffer concentration for TCP at different pH values. Reaction conditions: $[FAC]_0$ = 185 μM, $[TCP]_0$ = 2 μM, ionic strength = 0.1 M, T = 25°C. Error bars and uncertainties indicate 95% confidence intervals.

Electron paramagnetic resonance (EPR) spectroscopy

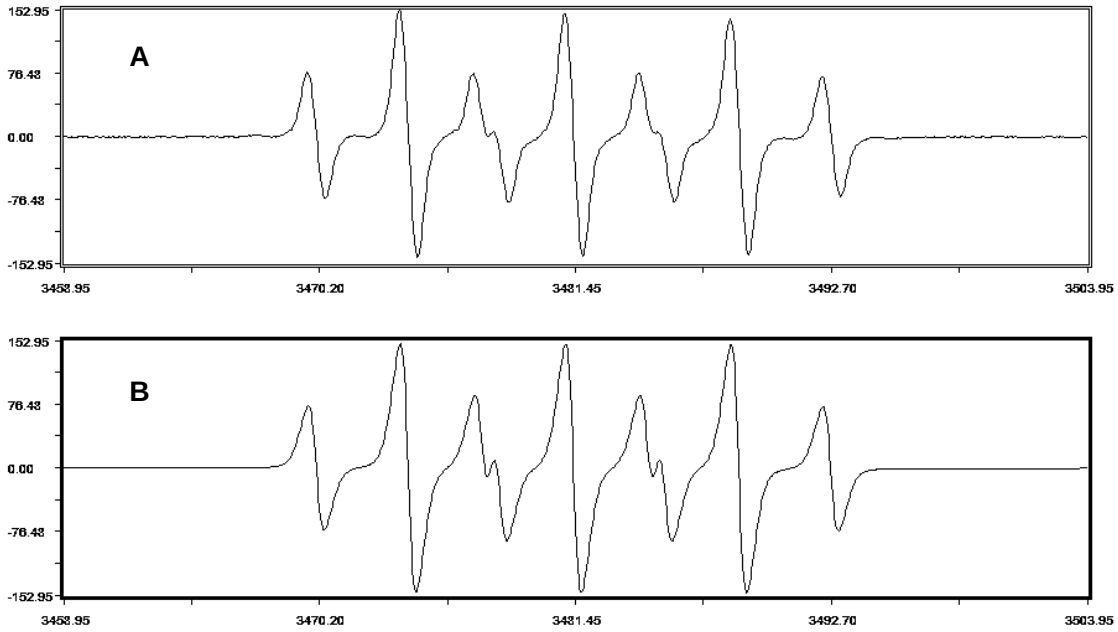

Figure S9. (A) EPR spectrum of a FAC solution (~100 μM) adjusted to pH < 3 with HNO_3 and mixed with 5,5-dimethyl-1-pyrroline-*N*-oxide (DMPO). EPR conditions: room temperature (~22°C), microwave frequency 9.78 GHz, microwave power 10 mW, modulation amplitude 1.0 G, time constant 81.9 ms, and conversion time 41 s. No signal was observed in the absence of DMPO. **(B)** Simulation of (A) in *WinSim 2002* using two radical species. Species 1 consists of one atom with spin 1 and a^{H} = 7.26 G. Species 2 consists of two atoms with spin ½ and a^{H} = 4.04 G.

Contributions of various reactions to k_{calc} for phenol

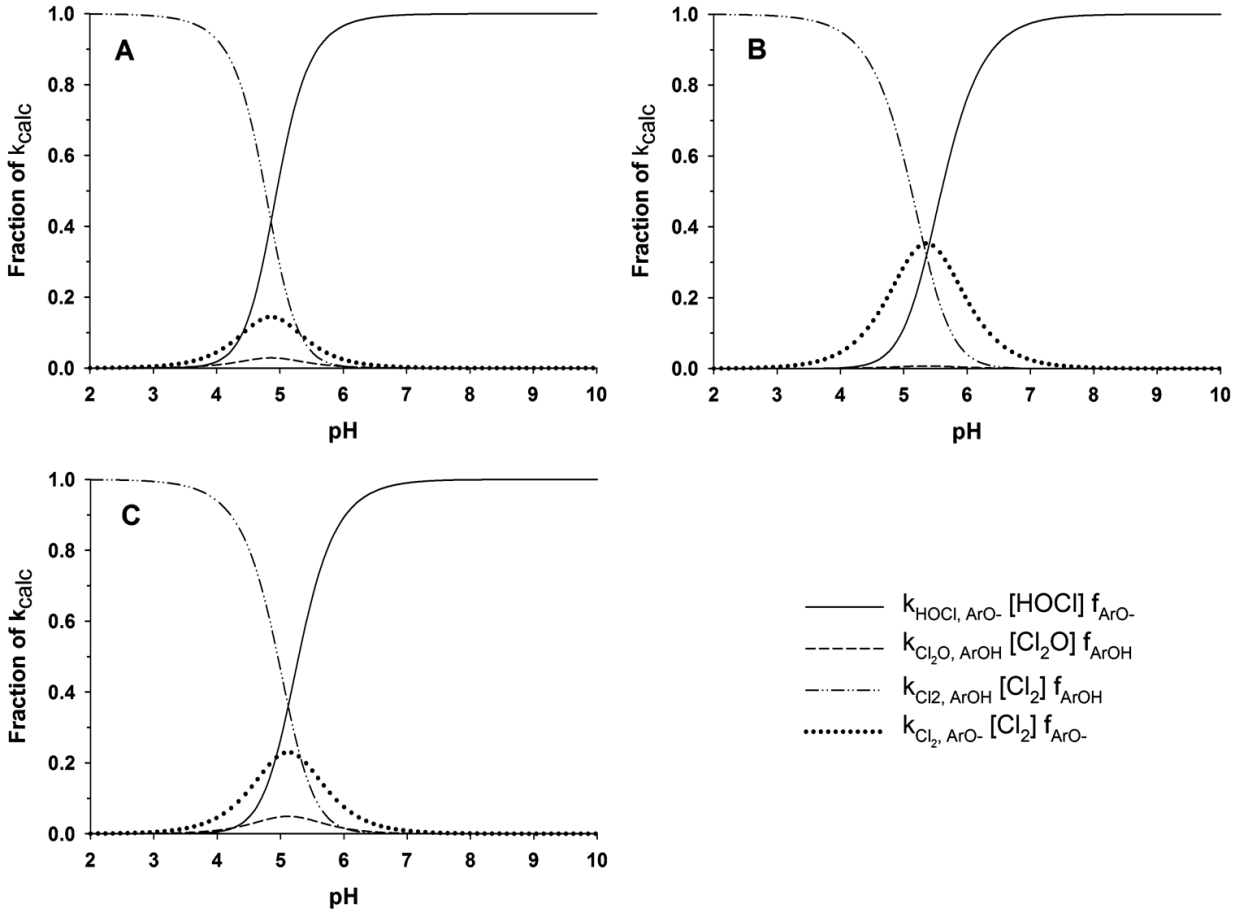

Figure S10. Contributions of Cl_2, Cl_2O, and HOCl to phenol reactivity (represented as fractions of k_{calc}) **(A)** under typical drinking water treatment conditions ([FAC] = 28 μM, [Cl^-] = 0.3 mM), **(B)** in the presence of excess chloride ([FAC] = 28 μM, [Cl^-] = 3 mM), and **(C)** under typical wastewater treatment conditions ([FAC] = 100 μM, [Cl^-] = 1 mM). ArOH and ArO^- denote the conjugate acid and phenolate forms, respectively.

Contributions of various reactions to k_{calc} for TCP

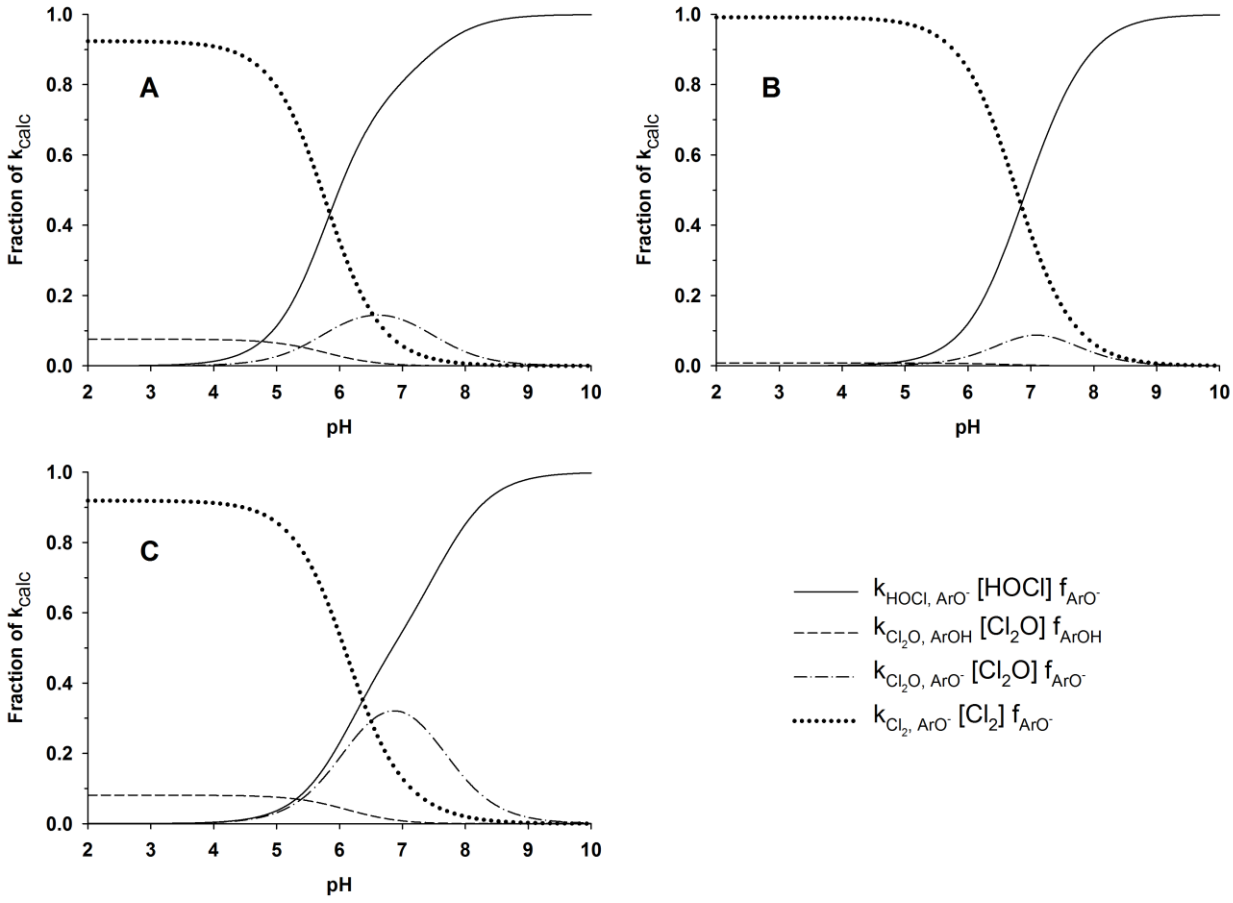

Figure S11. Contributions of Cl_2, Cl_2O, and HOCl to 2,4,6-trichlorophenol (TCP) reactivity (represented as fractions of k_{calc}) **(A)** under typical drinking water treatment conditions ([FAC] = 28 μM, $[Cl^-]$ = 0.3 mM), **(B)** in the presence of excess chloride ([FAC] = 28 μM, $[Cl^-]$ = 3 mM), and **(C)** under typical wastewater treatment conditions ([FAC] = 100 μM, $[Cl^-]$ = 1 mM). ArOH and ArO^- denote the conjugate acid and phenolate forms, respectively.

Contributions to k_{calc} for different (chloro)phenols

At a given pH, the fractions of k_{calc} contributed by reactions with Cl_2 and Cl_2O increase as the (chloro)phenol becomes more highly chlorinated and, thus, less reactive towards FAC (Fig. S12). This finding is consistent with the reactivity-selectivity principle.[12]

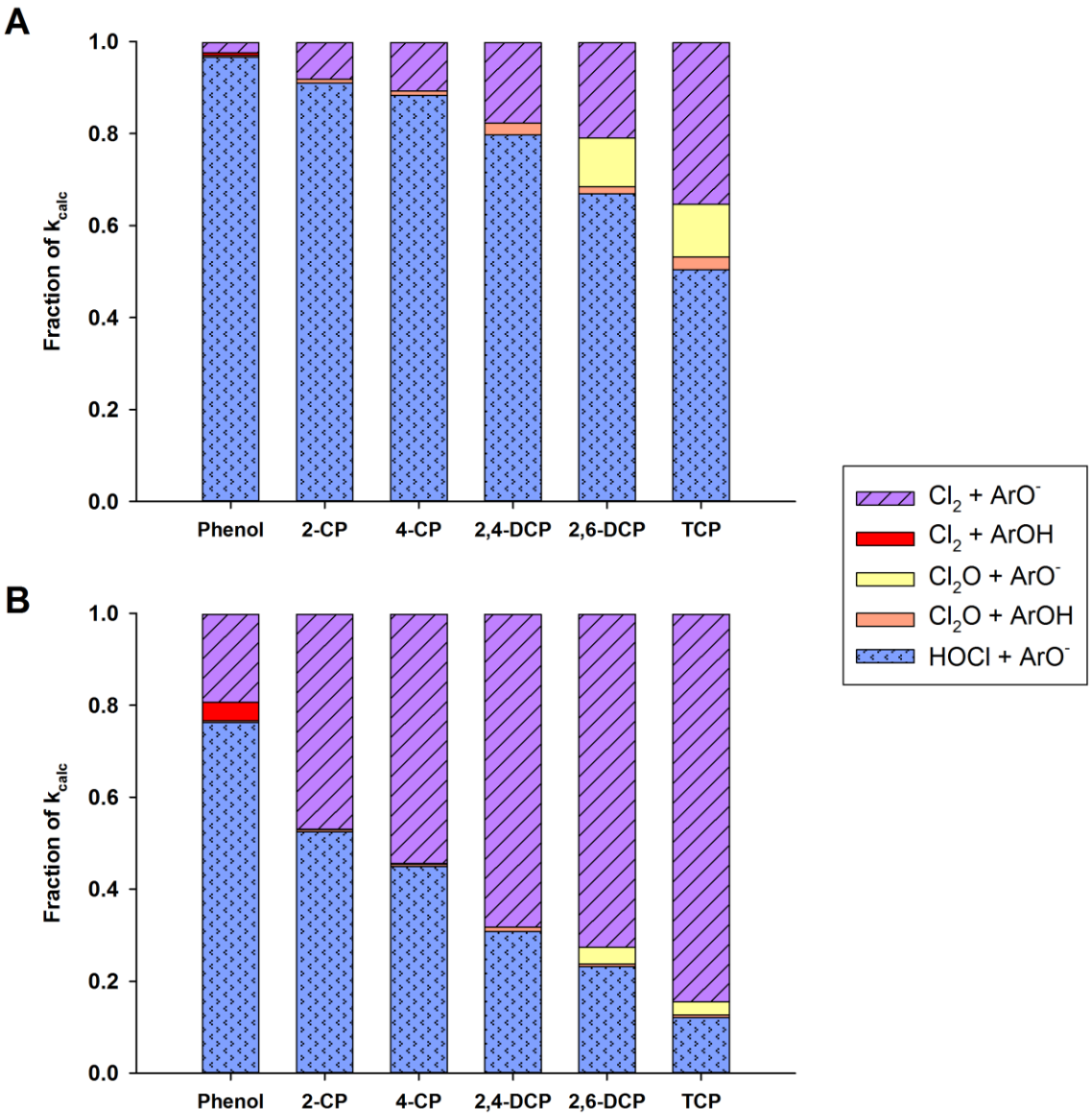

Fig. S12. Contributions of Cl_2, Cl_2O, and HOCl to overall (chloro)phenol reactivities in FAC (represented as fractions of k_{calc}) **(A)** under drinking water treatment conditions (pH 6, [FAC] = 28 µM, $[Cl^-]$ = 0.3 mM) and **(B)** in the presence of excess chloride (pH 6, [FAC] = 28 µM, $[Cl^-]$ = 3 mM). ArOH and ArO^- denote the conjugate acid and phenolate forms, respectively.

Calculating changes in [Cl_2]

Cl_2 and HOCl can be assumed to be in equilibrium in solutions of free available chlorine:

$$HOCl + H^+ + Cl^- \rightleftharpoons Cl_2 + H_2O$$

with k_1 as the rate constant of the forward reaction and k_{-1} as that of the reverse reaction. The equilibrium constant is represented by K_{Cl_2}.

The change in [Cl_2] over time can be written as the following:

$$\frac{d[Cl_2]}{dt} = k_1[HOCl][H^+][Cl^-] - k_{-1}[Cl_2] \quad (1)$$

Mass balance: $[HOCl] + [Cl_2] = [HOCl]_{eq} + [Cl_2]_{eq}$ (2)

Rearranging eq. 2: $[HOCl] = [HOCl]_{eq} + [Cl_2]_{eq} - [Cl_2]$ (3)

where $[HOCl]_{eq}$ and $[Cl_2]_{eq}$ represent the equilibrium concentrations of HOCl and Cl_2, respectively.

Substituting eq. 3 into eq. 1:

$$\frac{d[Cl_2]}{dt} = k_1\left([HOCl]_{eq} + [Cl_2]_{eq} - [Cl_2]\right)[H^+][Cl^-] - k_{-1}[Cl_2] \quad (4)$$

Expanding eq. 4:

$$\frac{d[Cl_2]}{dt} = k_1[H^+][Cl^-][HOCl]_{eq} + k_1[H^+][Cl^-][Cl_2]_{eq} - k_1[H^+][Cl^-][Cl_2] - k_{-1}[Cl_2] \quad (5)$$

The equilibrium constant K_{Cl_2} can be written as the following:

$$K_{Cl_2} = \frac{[Cl_2]_{eq}}{[HOCl]_{eq}[H^+][Cl^-]} \quad (6)$$

Rearranging eq. 6: $[HOCl]_{eq} = \frac{[Cl_2]_{eq}}{K_{Cl_2}[H^+][Cl^-]}$ (7)

Substituting eq. 7 into eq. 5:

$$\frac{d[Cl_2]}{dt} = k_1[H^+][Cl^-]\left(\frac{[Cl_2]_{eq}}{K_{Cl_2}[H^+][Cl^-]}\right) + k_1[H^+][Cl^-][Cl_2]_{eq} - k_1[H^+][Cl^-][Cl_2] - k_{-1}[Cl_2] \quad (8)$$

Canceling $[H^+]$ and $[Cl^-]$ in the first term on the right-hand side of eq. 8:

$$\frac{d[Cl_2]}{dt} = \left(\frac{k_1}{K_{Cl_2}}\right)[Cl_2]_{eq} + k_1[H^+][Cl^-][Cl_2]_{eq} - k_1[H^+][Cl^-][Cl_2] - k_{-1}[Cl_2] \quad (9)$$

Since $K_{Cl_2} = \frac{k_1}{k_{-1}}$, eq. 9 can be written as the following:

$$\frac{d[Cl_2]}{dt} = k_{-1}[Cl_2]_{eq} + k_1[H^+][Cl^-][Cl_2]_{eq} - k_1[H^+][Cl^-][Cl_2] - k_{-1}[Cl_2] \quad (10)$$

The right-hand side of eq. 10 is the product of two binomials:

$$\frac{d[Cl_2]}{dt} = (k_1[H^+][Cl^-] + k_{-1})\left([Cl_2]_{eq} - [Cl_2]\right) \quad (11)$$

At constant $[H^+]$ and $[Cl^-]$, the reaction becomes a reversible pseudo-first order reaction. Thus, eq. 11 can be written as the following:

$$\frac{d[Cl_2]}{dt} = k'\left([Cl_2]_{eq} - [Cl_2]\right) \quad (12)$$

where $k' = k_1[H^+][Cl^-] + k_{-1}$ (13)

A characteristic time for Cl_2 formation can then be defined as: $t_{char} = \frac{\ln 2}{k'}$ (14)

Wang and Margerum[13] reported the following values for k_1 and k_{-1}:

$k_1 = 2.14\ (\pm 0.08)\times 10^4\ M^{-2}\ s^{-1}$
$k_{-1} = 22.3\ (\pm 0.6)\ s^{-1}$

Assuming $[Cl^-]$ = 0.17 mM (the lowest $[Cl^-]$ encountered in our experiments), t_{char} = 0.03 s at pH 2–12. As this characteristic time is much shorter than the duration of our phenol chlorination experiments, Cl_2 should not become depleted, even though its concentration is much lower than the initial concentrations of our (chloro)phenols.

Literature cited

1. Bichsel, Y.; von Gunten, U. Determination of iodide and iodate by ion chromatography with postcolumn reaction and UV/visible detection. *Anal. Chem.* **1999,** *71*, 34-38.

2. Sivey, J. D.; McCullough, C. E.; Roberts, A. L. Chlorine monoxide (Cl_2O) and molecular chlorine (Cl_2) as active chlorinating agents in reaction of dimethenamid with aqueous free chlorine. *Environ. Sci. Technol.* **2010,** *44*, 3357-3362.

3. Sivey, J. D.; Roberts, A. L. Assessing the reactivity of free chlorine constituents Cl_2, Cl_2O, and HOCl toward aromatic ethers. *Environ. Sci. Technol.* **2012,** *46*, 2141-2147.

4. Black & Veatch Corporation. *White's Handbook of Chlorination and Alternative Disinfectants*. 5th ed.; John Wiley & Sons: Hoboken, New Jersey, 2010.

5. Cherney, D. P.; Duirk, S. E.; Tarr, J. C.; Collette, T. W. Monitoring the speciation of aqueous free chlorine from pH 1 to 12 with Raman spectroscopy to determine the identity of the potent low-pH oxidant. *Appl. Spectrosc.* **2006,** *60*, 764-772.

6. Greenberg, A. E.; Clesceri, L. S.; Eaton, A. D. *Standard Methods for the Examination of Water and Wastewater*. 18th ed.; American Public Health Association, American Water Works Association, Water Environment Federation: Washington, DC, 1992.

7. Israel, G. C. The kinetics of chlorohydrin formation. Part II. The reaction between hypochlorous acid and allyl alcohol in the presence of sodium acetate-acetic acid buffers of constant pH. *J. Chem. Soc.* **1950**, 1286-1289.

8. Anbar, M.; Dostrovsky, I. Ultra-violet absorption spectra of some organic hypohalites. *J. Chem. Soc.* **1954**, 1105-1108.

9. Chung, A.; Israel, G. C. The kinetics of chlorohydrin formation. Part VIII. The reaction between hypochlorous acid and allyl acetate in the presence of sodium acetate-acetic acid buffers of constant pH. *J. Chem. Soc.* **1955**, 2667-2673.

10. de la Mare, P. B. D.; Hilton, I. C.; Varma, S. The kinetics and mechanisms of aromatic halogen substitution. Part IX. Mixtures of acetic acid and aqueous hypochlorous acid. *J. Chem. Soc.* **1960**, 4044-4054.

11. Jia, Z.; Margerum, D. W.; Francisco, J. S. General-acid-catalyzed reactions of hypochlorous acid and acetyl hypochlorite with chlorite ion. *Inorg. Chem.* **2000,** *39*, 2614-2620.

12. Anslyn, E. V.; Dougherty, D. A. Modern Physical Organic Chemistry. University Science: 2006; pp 377-378.

13. Wang, T. X.; Margerum, D. W. Kinetics of reversible chlorine hydrolysis: Temperature dependence and general-acid/base-assisted mechanisms. *Inorg. Chem.* **1994,** *33*, 1050-1055.